

# MicroRNA-22 enhances radiosensitivity in cervical cancer cell lines via direct inhibition of c-Myc binding protein, and the subsequent reduction in hTERT expression

MAYUMI NAKAMURA<sup>1</sup>, MASAMI HAYASHI<sup>1</sup>, HIROMI KONISHI<sup>1</sup>, MISA NUNODE<sup>1</sup>, KEISUKE ASHIHARA<sup>1</sup>, HIROSHI SASAKI<sup>1</sup>, YOSHITO TERAJ<sup>2</sup> and MASAHIDE OHMACHI<sup>1</sup>

<sup>1</sup>Department of Obstetrics and Gynecology, Osaka Medical College, Takatsuki, Osaka 569-8686;

<sup>2</sup>Department of Obstetrics and Gynecology, Kobe University Graduate School of Medicine, Kobe, Hyogo 650-0017, Japan

Received September 9, 2019; Accepted December 19, 2019

DOI: 10.3892/ol.2020.11344

**Abstract.** MicroRNAs (miRs) influence the expression of their target genes post-transcriptionally and serve an important role in multiple cellular processes. The downregulation of miR-22 is associated with a poor prognosis in cervical cancer. However, the mechanisms underlying miR-22-mediated gene regulation and its function are yet to be elucidated. In the present study, the effect of miR-22 expression on the radiosensitivity of cervical cancer was investigated. First, miR-22 was either up- or downregulated to evaluate the regulation of the MYC-binding protein (MYCBP) in four cervical cancer cell lines (C-4I, SKG-II and SiHa). Notably, MYCBP expression was inversely associated with miR-22 induction. A dual-luciferase reporter gene assay revealed that miR-22 directly targets the MYCBP 3'-untranslated region. Subsequently, the level of human telomerase reverse transcriptase component (hTERT; an E-box-containing c-Myc target gene) was analyzed after the up- or downregulation of miR-22. Notably, miR-22-mediated repression of MYCBP reduced hTERT expression. In addition, the influence of miR-22 on radiosensitivity in C-4I, SKG-II and SiHa cells was examined using a clonogenic assay and in mouse xenograft models. Upregulation of miR-22 was associated with increased radiosensitivity. Furthermore, lentiviral transduction of miR-22 reduced the Ki-67 index while increasing the TUNEL index in xenograft tissue. The current findings indicate the potential utility of miR-22 in radiotherapy for cervical cancer.

## Introduction

Cervical cancer is responsible for 570,000 cases and 311,000 deaths in 2018 worldwide, ranking in the fourth most common cancer affecting women (1). Although early screening has aided in reducing the death rates, there is an increased prevalence in patients aged between 20 and 40 years has been observed (2). The age-adjusted incidence rate in the cervical adenocarcinoma cases aged 39 or younger has significantly increased from 1976 to 2012 (annual percent change=5.0) in Japan (2). In the United States, cervical cancer is currently most frequently diagnosed among women aged 35 to 44 years compared with those aged 45 to 54 years in the 1990s (3). Furthermore, the prognosis of advanced cervical cancer remains poor (4). The 5-year survival rate in the 2018 FIGO staging system is 85.6% for stage I tumors. In contrast, the 5-year survival rate for stage III and IV is 39.3 and 24.0%, respectively (5). Therefore, novel therapeutic interventions for advanced cervical cancer may confer improved outcomes for patients.

Human telomere reverse transcriptase (hTERT) is a catalytic subunit of telomerase that has been reported to regulate telomerase activity and serve a critical role in the tumorigenesis and the proliferation of cancer cells (6). Several recent studies demonstrated that expression of hTERT is elevated in a variety of cancers such as esophageal cancer (7) and thyroid carcinoma (8). Notably, downregulation of hTERT gene expression has been reported to enhance radiosensitivity in cervical cancer cells (9). The c-Myc proto-oncogene is a key switch for induced telomerase activity, including the upregulation of the hTERT gene (10).

MicroRNAs (miRNAs/miRs) are single-stranded RNA molecules of 21-25 base pairs. miRNA molecules bind to the complementary 3'-untranslated regions (UTRs) of target mRNAs and suppress gene expression via inhibition of the translation of its target mRNA (11). Accumulating evidence has indicated that miRNAs are implicated in a variety of diseases, such as cancer (12), cardiovascular disease (13) and metabolic disorders (14). A recent report revealed that decreased expression levels of miR-22 is associated with a poor prognosis in patients with cervical cancer (15). However, the role of miR-22 in the treatment of cervical

---

*Correspondence to:* Dr Masami Hayashi, Department of Obstetrics and Gynecology, Osaka Medical College, 2-7 Daigakumachi, Takatsuki, Osaka 569-8686, Japan  
E-mail: gyn122@osaka-med.ac.jp

**Key words:** microRNA, cervical cancer, radiotherapy, MYC binding protein, c-Myc, human telomerase reverse transcriptase

cancer is poorly characterized. In a previous study, miR-22 was identified as a tumor suppressor through the direct repression of MYC-binding protein (MYCBP) and subsequent reduction of downstream c-Myc-mediated molecules, which include cyclin D2, cyclin-dependent kinase 4, ornithine decarboxylase, lactate dehydrogenase-A, carbamoyl phosphate synthase-aspartate transcarbamylase-dihydroorotase, nucleolin and eukaryotic translation initiation factor 2A (16). However, the association between miR-22 and hTERT expression is yet to be elucidated.

In the present study, the effect of miR-22 expression on its downstream target (MYCBP) was investigated in cervical cancer cells. Moreover, the influence of miR-22 on the subsequent hTERT repression was subsequently examined. In addition, the biological role of miR-22 in radiosensitivity of cervical cancer cells was also investigated.

## Materials and methods

**Cell line.** The human cervical cancer cell lines C-4I, and SiHa were purchased from the American Type Culture Collection. SKG-II was provided by Keio University (Tokyo, Japan). Cells were cultured in DMEM (Gibco; Thermo Fisher Scientific, Inc.) supplemented with 10% fetal bovine serum (FBS) (Equitech-Bio, Inc.) at 37°C in a humidified incubator with 5% CO<sub>2</sub>.

**Transfection of precursor miRNA.** Pre-miR<sup>TM</sup> miRNA precursor molecules (pre-miR-22-3p; cat. no. AM17101), negative (non-specific) control (pre-miR-negative control #1; cat. no. AM17110) and inhibitor miRNA (anti-miR-22-3p; cat. no. AM17001) were ordered from Ambion (Thermo Fisher Scientific, Inc.). These were designed to mimic endogenous mature miRNAs, but the sequences are not publicly available. The mature miRNA sequence of miR-22-3p is 5'-AAG CUGCCAGUUGAAGAACUGU-3'. Cervical cancer cells were transfected with pre-miR-22-3p, anti-miR-22-3p or pre-miR-negative control (30 nM) for 24 h. Oligonucleotide transfection was performed using siPORT NeoFX Transfection Agent (Ambion; Thermo Fisher Scientific, Inc.).

**3'UTR reporter assay.** C-4I and SiHa cells were used for the 3'UTR reporter assay. The full length MYCBP 3'UTR was inserted downstream of a Gaussia luciferase (Gluc) reporter in the pEZX-MT05 vector (GeneCopoeia, Inc.). The secreted alkaline phosphatase (seAP) reporter gene was also present in the vector as an internal control for transfection normalization. As a control (pEZX-MT05-CT), miRNA target clone control vector (CmiT000001-MT05) was purchased from GeneCopoeia, Inc. Cells (1x10<sup>5</sup>/ml) seeded in 24-well plates were co-transfected using Lipofectamine<sup>®</sup> 2000 (Invitrogen; Thermo Fisher Scientific, Inc.) complexed with the pEZX-MT05 vector and pre-miR-22-3p, anti-miR-22-3p or pre-miR-negative control (cont miR) according to the manufacturer's protocol. Culture medium (DMEM, Gibco; Thermo Fisher Scientific, Inc.) was collected after 48 h and the relative luciferase activity (Gluc:seAP ratio) was analyzed using the Secrete-Pair Dual Luminescence Assay kit (GeneCopoeia, Inc.) according to the manufacturer's protocol.

**Bioinformatic analysis.** The putative human target genes of miR-22 were analyzed using the TargetScan (version 6.0; targets.org/) and miRDB (version 5.0; mirdb.org/) web-based bioinformatics algorithms. TargetScan predicts biological targets of miRNAs by searching for the presence of conserved 8mer, 7mer and 6mer sites that match the seed region of each miRNA (17). The cumulative weighted context ++ score <-0.1 was applied as the cut-off criteria (17). In miRDB, the prediction of miRNA-mRNA pair is based on both the 3'UTR and 5'UTR regions of conserved and non-conserved genes, the base composition in the regions flanking the seed pairing sites, secondary structure, and the location of the site within the 3'UTR (18).

**RNA and miRNA extraction and reverse transcription-quantitative (RT-q)PCR.** Total RNA was extracted from C-4I, SKG-II and SiHa cells using a RNeasy kit (Qiagen, Inc). A Super Script II Reverse Transcriptase kit (Invitrogen; Thermo Fisher Scientific, Inc.) was used to synthesize cDNA using random primers according to the manufacturer's protocol. A total of 1 µg of RNA, 125 ng random primers and 1 µl 10 mM dNTPs in 12 µl total volume were denatured at 65°C for 5 min before 2 min on ice. Then, 4 µl 5x first strand buffer and 2 µl of 0.1 M DTT were added followed by 1 µl Superscript II. Reactions were incubated 10 min at 25°C, 42°C for 50 min and 70°C for 15 min. Subsequently, TaqMan qPCR was performed in triplicate using the StepOne Real-Time PCR system (Applied Biosystems; Thermo Fisher Scientific, Inc.). The mixed primers for TaqMan qPCR used in the present study were purchased from Applied Biosystems in the form of a probe mix (MYCBP: Hs 00429315\_g1; c-Myc: Hs00153408\_m1; hTERT: Hs00972650\_m1) and GAPDH (Hs02786624\_g1, Applied Biosystems) was used as a housekeeping control gene. The sequences of these primers are not publicly available. PCR conditions were 95°C for 10 min, followed by 60°C for 1 min for 40 cycles following the manufacturer's protocol.

miRNA extraction was performed using a mirVana miRNA isolation kit (Invitrogen; Thermo Fisher Scientific, Inc.) according to the manufacturer's instructions. miRNA was then reverse transcribed using the microRNA reverse transcription kit according to the manufacturer's protocol (Applied Biosystems; Thermo Fisher Scientific, Inc.) in combination with the stem-loop primer for miR-22-3p (5'-GGCUGAGCCGAGUAGUUCU CAGUGGCAAGCUUUAUGUCCUGACCCAGCUAAAGCU GCCAGUUGAAGAACUGUUGCCCUCUGCC-3') and the endogenous control RNU48 (5'-GATGACCCAGGTA ACTCT GAGTGTGTCGCTGATGCCATCACCCGACGCTCTGA CC-3') (Applied Biosystems; Thermo Fisher Scientific, Inc.) and served as a template for the quantification of the expression of mature miRNA. qPCR of miR-22 was performed according to the manufacturer's instructions (Applied Biosystems; Thermo Fisher Scientific, Inc.). PCR conditions were 95°C for 10 min, followed by 60°C for 1 min for 40 cycles. Data analyses were performed using the 2<sup>-ΔΔC<sub>q</sub></sup> method (19).

**Western blot analysis.** Western blot analysis was performed as described previously (20). In brief, total proteins from C-4I, SKG-II and SiHa were prepared using Pierce RIPA Buffer (Thermo Fisher Scientific, Inc.). The protein concentration was quantified by DC Protein Assay (Bio-Rad Laboratories,

Inc.). Protein samples (15 µg/lane) were separated using 4-15% gradient gel electrophoresis (Bio-Rad Laboratories, Inc.) and transferred to PVDF membranes. After being blocked with 10% bovine serum albumin (New England BioLabs, Inc.) for 1 h at room temperature, the membranes were incubated overnight at 4°C with primary antibodies diluted at 1:200 (anti-MYCBP: Sigma-Aldrich, HPA041188) or 1:1,000 (anti-MYC: Cell Signaling, 13987 and anti-hTERT; LifeSpan BioSciences, Inc., LS-B11086). After 1 h incubation with horseradish peroxidase-conjugated anti-rabbit secondary antibody (1:4,000; goat anti-rabbit IgG; sc-2030; Santa Cruz Biotechnology, Inc.) at room temperature, the blots were visualized using enhanced chemiluminescence (ECL Plus; GE Healthcare Life Sciences).

**Clonogenic assay.** The clonogenic assay was performed using the technique described previously by Franken *et al* (21). In brief, C-4I and SKG-II cells ( $1.0 \times 10^2$ /well for 2 Gy- $2.4 \times 10^3$ /well for 8 Gy) transfected with miR-22, anti-miR-22 or cont miR were plated onto 6-well plates. Each group of cells was irradiated with various doses of X-ray (0, 2, 4, 6 and 8 Gy) from an X-ray generator (M-150WE; Softex Co., Ltd.) and incubated at 37°C in a humidified incubator with 5% CO<sub>2</sub> for 14 days. Fixation and staining of colonies was performed using a mixture of 0.5% crystal violet in methanol for 30 min at room temperature. Plates were rinsed with water and left to dry at room temperature. Counting of colonies was done on the following day. The cell survival was measured by standard colony formation after radiation treatment. Colonies containing >50 cells counted under a light microscope (CK40-F100, Olympus) at x40 magnification were defined as derived from clonogenically viable cells. The survival fraction of the cells was calculated by normalizing the plating efficiency of treated cells by that of control cells as described previously (21). Each experiment was performed at least three times in triplicate wells.

**Lentivirus infection.** Lentivirus ( $1 \times 10^7$  plaque forming units/ml) expressing LentimiRa-GFP-hsa-miR-22-3p (L-miR22-C-4I; cat. no. mh15295) and Lenti-III-miR-GFP Control (L-cont-C-4I; cat. no. m002) were purchased from Applied Biological Materials, Inc. Lentiviral transduction was conducted at a multiplicity of infection of 200 with a ViraDuctin Lentivirus Transduction kit (Cell Biolabs, Inc.), according to the manufacturer's protocol. In brief,  $5.0 \times 10^4$  C-4I cells were seeded in 24-well plates overnight at 37°C in a humidified incubator with 5% CO<sub>2</sub>. LentimiRa-GFP-hsa-miR-22-3p or Lenti-III-miR-GFP Control was added to the cells. After 48 h, purification was performed using puromycin until antibiotic-resistant colonies were identified. Post-transfection cells were further selected in DMEM (Gibco; Thermo Fisher Scientific, Inc.) containing puromycin for 2 weeks to establish stably transduced cells.

**A tumor xenograft assay.** Female 6-week-old athymic nude mice (BALB/c<sup>nu/nu</sup>) (average body weight 16 g) were purchased from Japan SLC, Int. A total of 10 animals were divided into two groups, each consisting of 5 mice (n=5). Mice were housed under standard environmental conditions at Osaka Medical College Division of Research Animal Laboratory (temperature, 22°C; humidity, 40-60%; light/dark cycle, 12 h

light 12 h darkness) with *ad libitum* access to food and water. All of the animal studies were carried out in compliance with the guidelines of the Osaka Medical College Animal Care and Use Committee, and followed the institutional guidelines for animal welfare and experimental conduct. Mice were monitored daily for signs of discomfort and pain by laboratory personnel as well as by the staff at the Division of Research Animal Laboratory. In addition to the pathological status, the mice were monitored to ensure that a humane endpoint was reached (defined as complete inability to ambulate). All mice gained weight over the entire study period while appearing generally healthy throughout the experiments. Under anesthesia with 2% isoflurane, C-4I cells infected with L-miR22-C-4I or L-cont-C-4I were injected subcutaneously into the flanks of nude mice ( $4 \times 10^6$  cells in 100 µl PBS per mouse).

The *in vivo* growth of C-4I xenografts was monitored by measuring their volumes and calculated using the modified ellipse formula (volume=length x (width)<sup>2</sup>/2). When the xenograft volumes reached ~100 mm<sup>3</sup>, the tumor was irradiated with X-rays (6 Gy) following the intraperitoneal administration of a mixture of three anesthetic agents (0.3 mg/kg medetomidine, 4 mg/kg midazolam and 5 mg/kg butorphanol). After irradiation, the tumors were measured with calipers every 7 days. A total of 35 days after irradiation, all mice were euthanized by cervical dislocation under anesthesia with 5% isoflurane for sample collection. Death was verified by the absence of a heart beat and the onset of rigor mortis. The tumors were excised, weighed (the maximum percentage of tumor weight of total body weight was <0.15%) and fixed in 10% neutral buffered formalin for 24 h at room temperature, and 4 µm-thick paraffin sections were prepared for immunohistochemistry and the terminal deoxynucleotidyl transferase dUTP nick-end labeling (TUNEL) assay.

**Immunostaining.** The aforementioned section from paraffin-embedded xenograft tissues were subjected to immunostaining. Tissue samples were formalin-fixed and embedded in paraffin. Deparaffinized and rehydrated sections were autoclaved in 0.01 mol/l citrate buffer (pH 6.0) for 15 min at 121°C for antigen retrieval. The endogenous peroxidase activity was blocked with 0.3% hydrogen peroxide solution in methanol for 30 min at room temperature, then sections were incubated at room temperature for 30 min with rabbit anti-Ki67 antibody (1:300; AB9260; Merck KGaA). The sections were then washed once with phosphate-buffered saline (PBS) and incubated with secondary antibody Histofine Simple Stain MAX PO (MULTI) (ready to use; cat. no. 414151F; Nichirei Corporation) for 30 min at room temperature. Finally, the sections were washed once with PBS and visualized by incubating with H<sub>2</sub>O<sub>2</sub>/diaminobenzidine substrate solution for 5 min. The sections were counterstained with hematoxylin for 20 sec at room temperature prior to dehydration and mounting. The Ki-67 index and percentage of apoptotic cells reflected the percentage of the total number of tumor cells with nuclear staining in viable regions per 5 high-power fields using a fluorescence microscope (BZ-X700, KEYENCE) at x400 magnification.

**TUNEL assay.** Apoptotic cell death was determined by TUNEL assay using a *in situ* Apoptosis Detection kit (Wako Pure

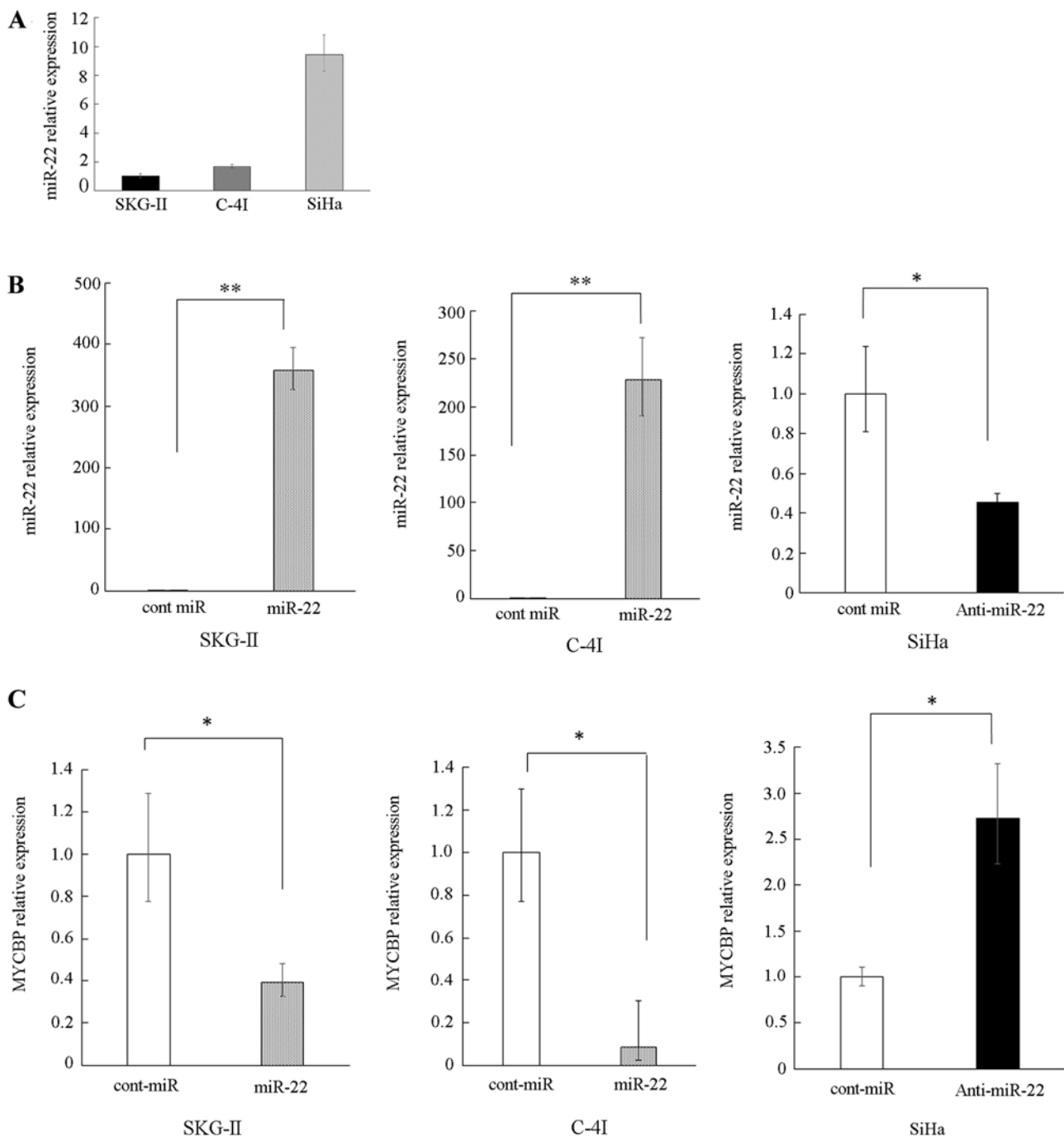


Figure 1. Inverse association between miR-22 and MYCBP in cervical cancer cell lines. (A) RT-qPCR of miR-22 expression levels in three cervical cancer cell lines. miR-22 relative expression levels were lowest in SKG-II cells therefore fold differences in miR-22 relative expression levels in C-4I and SiHa cells are presented relative to SKG-II cells. (B) SKG-II and C-4I cells were transfected with either precursor miR-22 or cont. SiHa cells were transfected with either inhibitor miR-22 or cont miR. The relative abundance of miR-22 normalized to RNU48 was calculated using RT-qPCR, and relative fold differences compared with cont miR are presented. (C) Overexpression of miR-22 inhibited MYCBP mRNA expression levels in SKG-II and C-4I cells. The suppression of miR-22 increased MYCBP mRNA expression levels in SiHa cells. Relative fold differences compared with cont miR are presented. Columns represent the mean  $\pm$  standard deviation. \* $P < 0.05$ , \*\* $P < 0.01$  vs. cont. miR, microRNA; MYCBP, MYC binding protein; RT-q, reverse transcription-quantitative; cont, control.

Chemical Industries, Ltd.), according to the manufacturer's protocol. The sections were deparaffinized for 10 min, dehydrated in 100% ethanol for 10 min and proteins of the sections were digested using pre-warmed protease solution for 5 min at 37°C. After washing, the sections were incubated with 50  $\mu$ l TdT reaction solution (consisting of TdT Enzyme 1  $\mu$ l + TdT Substrate Solution 49  $\mu$ l) for 10 min at 37°C. After washing, the endogenous peroxidase activity was blocked using 3% H<sub>2</sub>O<sub>2</sub>

for 5 min at room temperature. After washing, the sections were reacted with 100  $\mu$ l of POD-conjugated antibody solution for 10 min at 37°C. After removing the antibody solution and washing, immunoreactivity was visualized using 3,3'-diaminobenzidine. The sections were counterstained with 0.5% methyl green for 5 min at room temperature. The TUNEL index was calculated as the percentage of TUNEL-positive cells in 1,000 carcinoma cells in the areas of highest nuclear labeling under

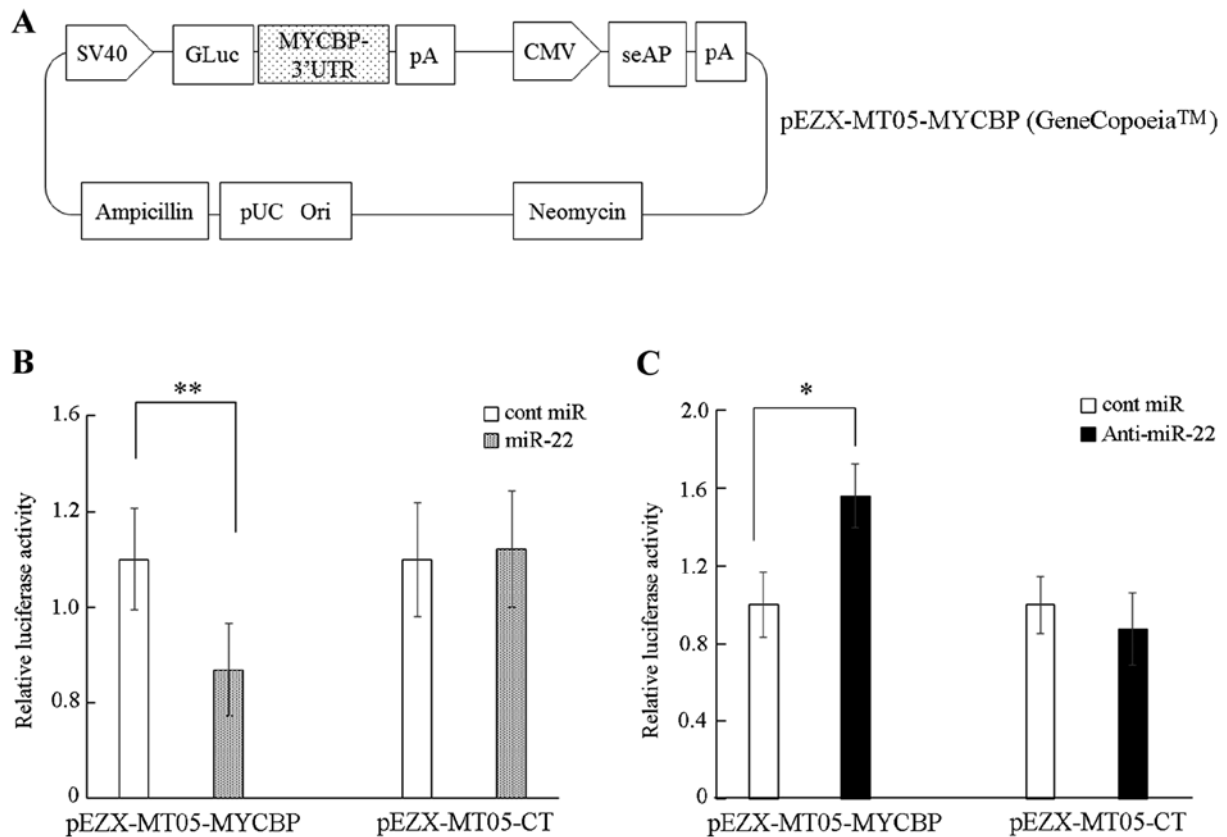


Figure 2. MYCBP is a direct target of miR-22. (A) A diagram of the MYCBP 3'UTR-containing reporter construct. (B) C-4I cells were co-transfected with the MYCBP 3'UTR reporter construct (pEZX-MT05-MYCBP) or control vector (pEZX-MT05-CT) and with miR-22 or control miR. Relative gaussian luciferase-to-seAP signal is shown. (C) SiHa cells were co-transfected with either pEZX-MT05-MYCBP or pEZX-MT05-CT and with either anti-miR22 or control. Data are exhibited as the mean  $\pm$  SD of three independent experiments. \* $P < 0.05$ , \*\* $P < 0.01$  vs. control. Columns represent the mean  $\pm$  standard deviation. miR, microRNA; MYCBP, MYC binding protein; 3'UTR, 3'untranslated region; cont/CT, control; seAP, secreted alkaline phosphatase; CMV, cytomegalovirus promoter; GLuc, Gaussia luciferase; pA, poly-A tail; pUC Ori, origin of replication.

a fluorescence microscope (BZ-X700, KEYENCE) at x400 magnification.

**Statistical analysis.** The statistical analyses were performed using the StatView software program (version 5.0; SAS Institute, Inc.). The data are presented as the mean  $\pm$  standard deviation of three independent experiments. The statistical analysis was performed using the Student's paired t-test and  $P < 0.05$  was considered to indicate a statistically significant difference.

## Results

**Overexpression of miR-22 suppresses the expression of MYCBP in cervical cancer cell lines.** RT-qPCR was performed to evaluate the expression profile of miR-22 in several cervical cancer cell lines. The endogenous miR-22 expression was higher in the SiHa cell line compared with the SKG-II and C-4I lines (Fig. 1A). Accordingly, SKG-II and C-4I were used for overexpression experiments of miR-22, whereas SiHa was used for reduced experiments of miR-22.

The overexpression of miR-22 was induced by the transfection of pre-miR-22, and an increased level of miR-22 in SKG-II and C-4I cells was confirmed (Fig. 1B). By contrast, the transfection of anti-miR-22 reduced the miR-22 expression level in SiHa cells (Fig. 1B).

Subsequently, it was determined whether or not expression of MYCBP could be altered by the overexpression or suppression of miR-22. RT-qPCR revealed that the level of MYCBP was decreased under conditions of miR-22 overexpression, while MYCBP mRNA was increased under conditions of miR-22 suppression (Fig. 1C).

**miR-22 directly targets MYCBP 3'UTR.** TargetScan and miRDB were utilized to predict that the MYCBP gene has a putative miR-22 target site at its 3'UTR region. To confirm that miR-22 directly targeted the MYCBP 3'UTR in cervical cancer cells, a luciferase reporter assay was performed. C-4I cells were co-transfected with either the precursor miRNA or control and with either a plasmid containing a luciferase reporter driven by the wild-type human MYCBP 3'UTR (pEZX-MT05-MYCBP; Fig. 2A) or a control plasmid (pEZX-MT05-CT). Treatment of C-4I with complexes of pre-miR-22 and pEZX-MT05-MYCBP significantly reduced the luciferase activity compared with that in the combination of cont miR and pEZX-MT05-MYCBP (Fig. 2B). Knockdown of miR-22 via the transfection of anti-miR22 significantly increased the luciferase activity of MYCBP 3'UTR compared with transfection of cont miR (Fig. 2C). The current results indicate that miR-22 suppresses the expression of MYCBP mRNA via direct targeting of the MYCBP 3'UTR in the cervical cancer cell lines.

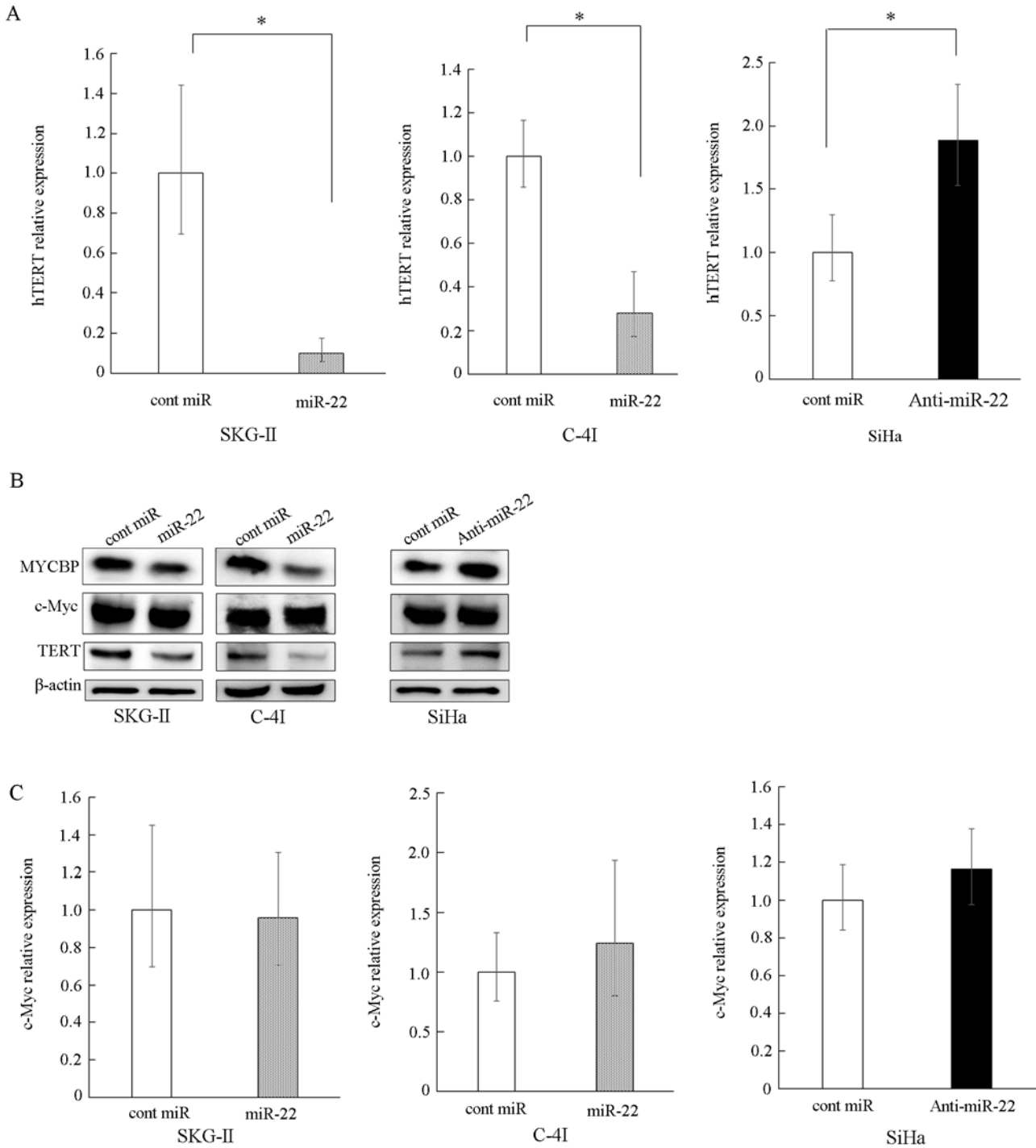


Figure 3. Effect of miR-22 on the expression of MYCBP, c-Myc and hTERT in cervical cancer cells. (A) SKG-II and C-4I cells were transfected with either miR-22 or cont miR. Overexpression of miR-22 inhibited hTERT mRNA expression levels in SKG-II and C-4I cells. SiHa cells were transfected with either anti-miR-22 or cont miR. The suppression of miR-22 expression increased hTERT mRNA expression levels in SiHa cells. The relative abundance of hTERT with respect to GAPDH was calculated using RT-qPCR, and the relative fold differences compared with cont miR are presented. (B) SKG-II and C-4I cells were transfected with cont miR or miR-22. SiHa cells were transfected with cont miR or anti-miR-22. The MYCBP, c-Myc, hTERT and β-actin (loading control) protein levels were detected using western blot analysis. (C) SKG-II and C-4I cells were transfected with either miR-22 or cont miR. SiHa cells were transfected with either anti-miR-22 or cont miR. Relative abundance of c-Myc with respect to GAPDH was calculated using RT-qPCR and the relative fold differences compared with cont miR are presented. Neither overexpression nor suppression of miR-22 significantly changed c-Myc mRNA expression levels. \*P<0.05 vs. control. miR, microRNA; MYCBP, MYC binding protein; RT-q, reverse transcription-quantitative; hTERT, human telomerase reverse transcriptase; cont, control.

*MYCBP regulates the expression of the c-Myc target gene hTERT.* MYCBP has been revealed to promote the activation of the c-Myc target gene via E-box (22). Therefore, the current study investigated whether or not the suppression

of MYCBP by miR-22 results in subsequent suppression of the E-box-dependent c-Myc target gene expression. The hTERT gene is an E-box-dependent target gene (23) and does not contain a predicted target site for miR-22 in its 3'UTR,

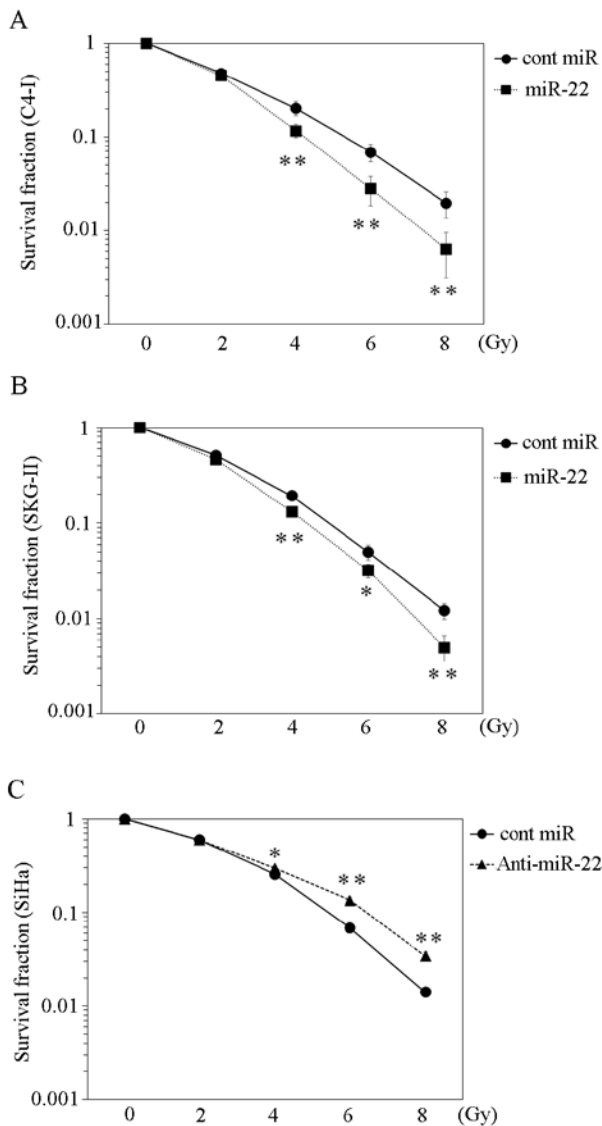


Figure 4. Effect of miR-22 on the radiosensitivity of cervical cancer cells *in vitro*. (A) C-4I and (B) SKG-II cells were transfected with miR-22 or cont miR. (C) SiHa cells were transfected with anti-miR-22 or cont miR. After transfection, the cells were irradiated with various doses of X-ray. \* $P < 0.05$ , \*\* $P < 0.01$ . miR, microRNA, cont, control.

according to TargetScan and miRDB. Thus, the effect of the overexpression or suppression of miR-22 on hTERT expression levels was examined. It was revealed that the overexpression of miR-22 significantly reduced the expression level of hTERT, whereas suppression of miR-22 increased hTERT expression (Fig. 3A and B).

Subsequently, whether or not the miR-22-induced hTERT suppression was dependent on the interaction of miR-22 with c-Myc 3'UTR was investigated, and *in silico* analyses using TargetScan and miRDB predicted that the c-Myc gene had no target site for miR-22. Moreover, RT-qPCR and western blot analyses revealed that neither the overexpression nor the suppression of miR-22 affected c-Myc levels at the mRNA or protein level (Fig. 3B and C). The present results do not support the possibility of a direct interaction between miR-22 and c-Myc mRNA, thus indicating that the inhibition of MYCBP by miR-22 resulted in the subsequent reduction of the c-Myc target gene hTERT.

*Increased miR-22 expression improves the radiosensitivity of cervical cancer cell lines in vitro.* Telomerase activity reportedly influences the radiosensitivity of the cervical cancer cell line SiHa (24). To investigate the effect of miR-22 on radiosensitivity, C-4I and SKG-II cells were transfected with miR-22 or control miRNA and irradiated with various radiation doses (2, 4, 6 and 8 Gy). Compared with the control miRNA, the survival fraction of the miR-22-transfected group was significantly lower (Fig. 4A and B). Conversely, SiHa cells with a suppressed miR-22 expression exhibited a higher survival fraction following irradiation compared with cells transfected with the control miRNA (Fig. 4C).

*A cervical cancer cell line transduced with miR-22 exhibits an improved radiosensitivity in vivo.* Given that the overexpression of miR-22 improved the radiosensitivity of cervical cancer cells by the subsequent reduction of hTERT, the therapeutic potential of miR-22 was assessed in a cervical cancer xenograft model. C-4I cells were stably transduced with lentiviruses containing precursor miR-22 (L-miR22) or control lentiviral vector (L-cont). Stable transduction efficiency was confirmed by the expression of GFP (Fig. 5A). Significant upregulation of miR-22 in L-miR22-transduced C-4I cells (L-miR22-C-4I) was confirmed using RT-qPCR (Fig. 5B). Transduced C-4I cells (L-miR22-C-4I or L-cont-C-4I) were injected subcutaneously, and then the tumor was irradiated with an X-ray dose of 6 Gy once the xenograft volume reached 100 mm<sup>3</sup>. The tumor growth was significantly inhibited in the L-miR22-C-4I mice compared with that in the L-cont-C-4I mice (between 7 days and 21 days after irradiation;  $P < 0.05$ , after 28 days or later;  $P < 0.01$ ), indicating that miR-22 had a radiosensitizing effect *in vivo* (Fig. 5C). A total of 35 days after irradiation, tumor nodules were excised and weighed (Fig. 5D). It was revealed that the L-miR22-C-4I tumors were significantly smaller compared with the L-cont-C-4I tumors ( $P < 0.05$ ; Fig. 5D). In addition, paraffin sections were prepared from the excised tumor and immunostaining of Ki-67 (Fig. 5E) was performed, in addition to a TUNEL assay (Fig. 5F), to investigate the effect on proliferation and apoptosis. The Ki-67 index was significantly lower in the L-miR22-C-4I tumor compared with that in the L-cont-C-4I tumor group ( $P < 0.05$ ; Fig. 5E). Furthermore, the TUNEL index was higher in the L-miR22-C-4I tumor group compared with that in the L-cont-C-4I tumor group, suggesting that miR-22 may influence apoptosis ( $P < 0.05$ ; Fig. 5F).

*Direct inhibition of MYCBP by miR-22 subsequently reduced hTERT expression.* The present study suggests a novel mechanism for direct miR-22 mediated suppression of MYCBP expression resulting in the subsequent reduction of c-Myc-mediated transactivation (Fig. 6).

## Discussion

In the present study, it was demonstrated that miR-22 directly inhibited MYCBP mRNA expression by targeting the 3'UTR of MYCBP and subsequently reduced the hTERT expression level in cervical cancer cells. Notably, the ectopic expression of miR-22 resulted in increased radiosensitivity both *in vitro* and *in vivo*.

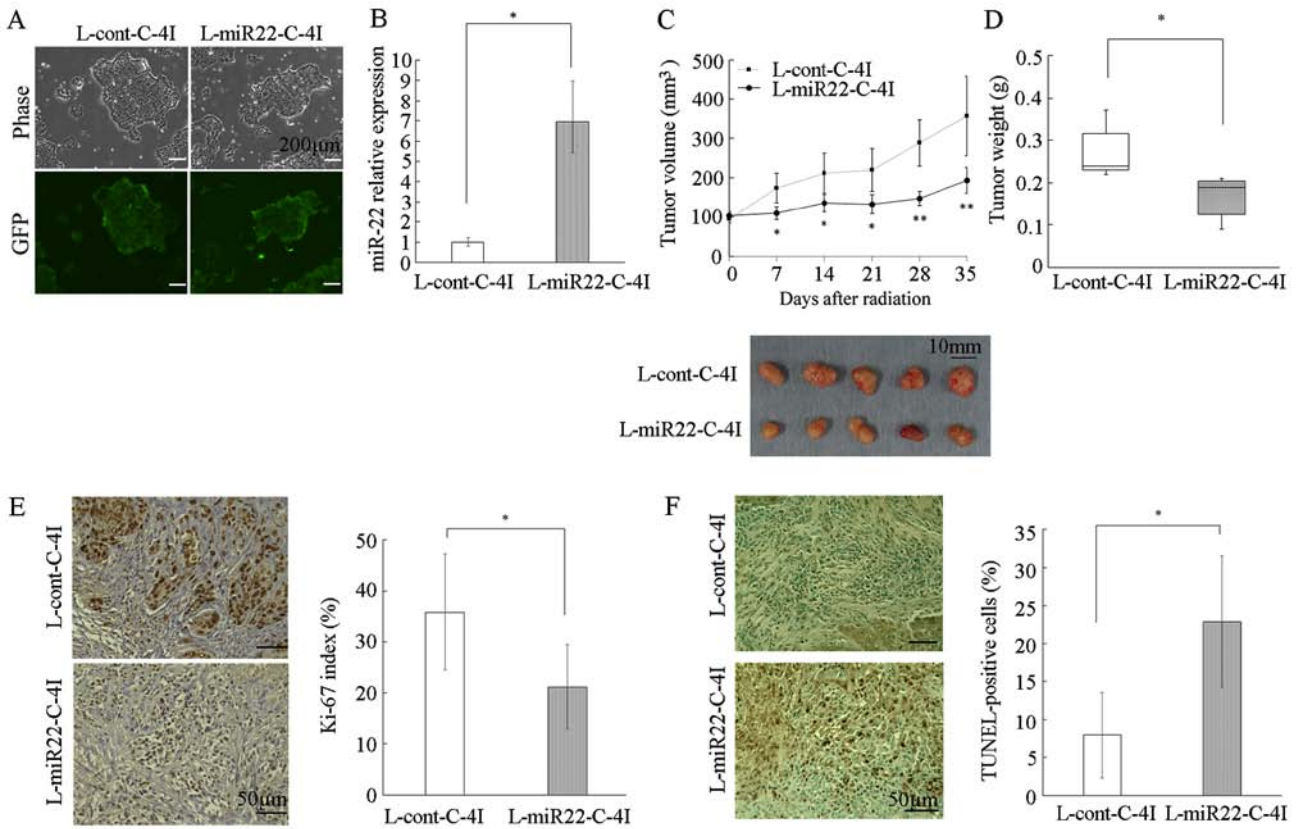


Figure 5. Effect of miR-22 on the radiosensitivity of cervical cancer cells in *in vivo* xenografts. (A) C-4I cells were infected with miR-22 lentivirus or control lentivirus, and selected using puromycin. Stably transfected C-4I cells were examined by phase-contrast microscopy (upper panel) and fluorescent microscopy (lower panel) (BZ-X700; Keyence Corporation). Magnification, x40. Scale bar=200  $\mu$ m. (B) miRNA was extracted from C-4I cells stably transfected with L-miR22-C-4I or with L-cont-C-4I. The relative abundance of miR-22 with respect to RNU48 was calculated using RT-qPCR, and relative fold differences compared with L-cont-C-4I are presented. (C) Transduced C-4I cells (L-miR22-C-4I or L-cont-C-4I) were injected into the flanks of nude mice. When tumors reached ~100 mm<sup>3</sup>, the mice received irradiation treatment (6 Gy). Tumor volume was measured once a week and each value represents the mean volume  $\pm$  SD. Tumor tissues removed from individual 5 mice in each group are shown. (D) Tumors were excised and weighed five weeks following irradiation treatment. Each column represent the mean tumor weight of the five mice  $\pm$  SD. (E) Immunostaining images indicate the Ki67 expression of tumor tissue imaged on BZ-X700 microscope (Keyence Corporation). The percentage of Ki67-positive nuclei in tumor cells was calculated from five fields arbitrarily selected. Magnification, x400. Bar=50  $\mu$ m. (F) Apoptosis of tumors was evaluated by TUNEL staining. Slides were imaged using a fluorescence BZ-X700 microscope (Keyence Corporation). The percentage of TUNEL-positive cells in tumor cells was calculated from five fields arbitrarily selected. Magnification, x400. Scale bar=50  $\mu$ m. \*P<0.05, \*\*P<0.01. miR, microRNA; GFP, green fluorescent protein; cont, control.

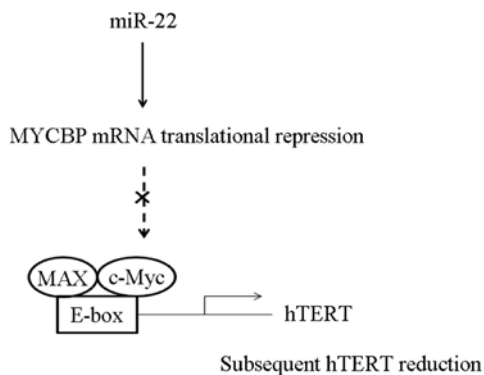


Figure 6. Schematic representation of the regulation of the MYCBP/c-Myc/hTERT axis by miR-22. miR-22 directly suppresses MYCBP, thus resulting in an impairment of the E-box-dependent hTERT expression. miR, microRNA; MYCBP, MYC binding protein; hTERT, human telomerase reverse transcriptase.

as miR-34 and miR-200 (12,25). miR-22 was originally identified from HeLa cells on chromosome 17p13 (26), and there is increasing evidence indicating that miR-22 serves a tumor suppressive role in various cancer types. For example, cervical cancer cell proliferation was attenuated by miR-22 via the inhibition of ATP citrate lyase, which is a key enzyme influencing metabolic activity (27). Furthermore, Li *et al* (28) reported a negative correlation between miR-22 expression level and the metastatic potential of ovarian cancer cells *in vitro* by analyzing the invasion of SKOV-3 cells. In gastric cancer, miR-22 suppressed invasion and metastasis via the inhibiting of matrix metalloproteinase 14 and Snail (29). Moreover, in colorectal cancer cells, miR-22 promoted apoptosis in response to 5-fluorouracil treatment (30) and a recent report indicated that a decrease in miR-22 expression in cervical cancer cells was associated with a poorer prognosis (15). These results highlight the potential utility of miR-22 as a therapeutic target in cancers.

It has previously been indicated that certain miRNAs serve as promoters of cancer progression such as miR-155 and miR-221, while others serve as tumor suppressors, such

miRNA has also been revealed to serve a central role in modulating the radiosensitivity of cervical cancer cells (31,32). The overexpression of miR-29b in SiHa and HeLa cells

promoted radiosensitivity via the targeting of phosphatase and tensin homolog deleted from chromosome 10 (31). Pedroza-Torres *et al* (32) reported that the overexpression of miR-125 sensitized the SiHa, CaSki and HeLa cell lines to radiation therapy, via the downregulation of cyclin-dependent kinase inhibitor 1. Recently, Zhang *et al* (33) determined that miR-22 improved radiosensitivity via targeting silent information regulator 1 in breast cancer cells. In bone marrow mesenchymal stem cells, miR-22 expression level was increased following irradiation, and served an important role in the generation of reactive oxygen species and subsequent apoptosis (34). These previous reports support the findings of the present study; miR-22 was revealed to enhance radiosensitivity and apoptosis following irradiation in cervical cancer cells. Notably, the present results indicated a novel mechanism by which miR-22 regulates the cellular response to radiation via the modulation of MYCBP and hTERT expression. It was observed that miR-22 suppressed MYCBP mRNA expression levels without a change in c-Myc in the MYCBP/c-Myc/hTERT axis. Bioinformatics analyses indicated a potential binding site of miR-22 to MYCBP, which was validated by luciferase reporter assays in the present study. On the other hand, *in silico* prediction resources, such as TargetScan and miRDB, indicated no potential binding site for miR-22 to c-Myc. In addition, Xing *et al* revealed that the knockdown of MYCBP using siRNAs had no significant impact on the c-Myc expression (16), which supports the present results.

The MYCBP gene encodes a protein of ~11 kDa, which binds the N-terminal region of c-Myc via its C-terminal domain and activates the E-box-dependent transcription activity of c-Myc (22,35,36). Previous studies have suggested that MYCBP is an important regulator affecting the progression and development of tumors; for example, in glioma cells, the MYCBP mRNA expression increased along with the malignant grade (36). Moreover, in gastric cancer, Gong *et al* (37) reported that MYCBP mRNA expression was markedly increased compared with that in normal gastric tissues and knockdown of MYCBP inhibited the metastatic capacity. However, the influence of MYCBP on radiosensitivity is yet to be elucidated. A limitation of the present study is that the association between MYCBP and hTERT was not investigated to determine whether it was direct or indirect.

In conclusion, the present findings not only revealed the molecular mechanisms of miR-22 in cervical cancer cells, but also highlighted a novel potential approach for radiotherapy through miR-22 in cervical cancer cells. To elucidate the mechanism underlying miR-22-mediated radio-sensitization in greater detail, it would be necessary to determine whether the association between MYCBP and hTERT is direct or indirect, and this should be investigated in a future study.

#### Acknowledgements

Not applicable.

#### Funding

The present study was supported by grants from the Japan Society for the Promotion of Science; (grant. nos. 25462619 and 17K11304).

#### Availability of data and materials

The datasets used and/or analyzed during the current study are available from the corresponding author upon reasonable request.

#### Authors' contributions

MNa and MH made substantial contributions to the conception and design of the study, acquisition of the data and/or statistical analyses and drafting of the manuscript. HK and KA contributed to the xenograft model assay. MNu was involved in the reporter assay experiments. YT, HS and MO performed review and editing of the manuscript and assisted with data analysis. All authors read and approved the final manuscript.

#### Ethics approval and consent to participate

The animal welfare guidelines for the care and use of laboratory animals were followed and experimental protocol was approved by The Osaka Medical College Animal Care and Use Committee.

#### Patient consent for publication

Not applicable.

#### Competing interests

The authors declare that they have no competing interests.

#### References

1. Bray F, Ferlay J, Soerjomataram I, Siegel RL, Torre LA and Jemal A: Global cancer statistics 2018: GLOBOCAN estimates of incidence and mortality worldwide for 36 cancers in 185 countries. *CA Cancer J Clin* 68: 394-424, 2018.
2. Yagi A, Ueda Y, Kakuda M, Tanaka Y, Ikeda S, Matsuzaki S, Kobayashi E, Morishima T, Miyashiro I, Fukui K, *et al*: Epidemiologic and clinical analysis of cervical cancer using data from the population-based Osaka cancer registry. *Cancer Res* 79: 1252-1259, 2019.
3. Fokom Domguez J and Schmeler KM: Conservative management of cervical cancer: Current status and obstetrical implications. *Best Pract Res Clin Obstet Gynaecol* 55: 79-92, 2019.
4. Chohen PA, Jhingran A, Oaknin A and Denny L: Cervical cancer. *Lancet* 393: 169-182, 2019.
5. Wright JD, Matsuo K, Huang Y, Tergas AI, Hou JY, Khoury-Collado F, St Clair CM, Ananth CV, Neugut AI and Hershman DL: Prognostic performance of the 2018 international federation of gynecology and obstetrics cervical cancer staging guidelines. *Obstet Gynecol* 134: 49-57, 2019.
6. Pal J, Gold JS, Munshi NC and Shamma MA: Biology of telomeres: Importance in etiology of esophageal cancer and as therapeutic target. *Transl Res* 162: 364-370, 2013.
7. Lord RV, Salonga D, Danenberg KD, Peters JH, DeMeester TR, Park JM, Johansson J, Skinner KA, Chandrasoma P, DeMeester SR, *et al*: Telomerase reverse transcriptase expression is increased early in the Barrett's metaplasia, dysplasia, adenocarcinoma sequence. *J Gastrointest Surg* 4: 135-142, 2000.
8. Hoang-Vu C, Boltze C, Gimm O, Poremba C, Dockhorn-Dworniczak B, Köhrle J, Rath FW and Dralle H: Expression of telomerase genes in thyroid carcinoma. *Int J Oncol* 21: 265-272, 2002.
9. Wang R, Lin F, Wang X, Gao P, Dong K, Wei SH, Cheng SY and Zhang HZ: The therapeutic potential of survivin promoter-driven siRNA on suppressing tumor growth and enhancing radiosensitivity of human cervical carcinoma cells via downregulating hTERT gene expression. *Cancer Biol Ther* 6: 1295-1301, 2007.

10. Kyo S, Takakura M, Taira T, Kanaya T, Itoh H, Yutsudo M, Ariga H and Inoue M: Spl cooperates with c-Myc to activate transcription of the human telomerase reverse transcriptase gene (hTERT). *Nucleic Acids Res* 28: 669-677, 2000.
11. Ambros V: MicroRNAs: Tiny regulators with great potential. *Cell* 107: 823-826, 2001.
12. Rupaimoole R and Slack FJ: MicroRNA therapeutics: Towards a new era for the management of cancer and other diseases. *Nat Rev Drug Discov* 16: 203-222, 2017.
13. Kaur A, Mackin ST, Schlosser K, Wong FL, Elharram M, Delles C, Stewart DJ, Dayan N, Landry T and Pilote L: Systematic review of microRNA biomarkers in acute coronary syndrome and stable coronary artery disease. *Cardiovasc Res*: pii: cvz302, 2019 (Epub ahead of print).
14. Ji C and Guo X: The clinical potential of circulating microRNAs in obesity. *Nat Rev Endocrinol* 15: 731-743, 2019.
15. Zhang L, Chen B and Ding D: Decreased microRNA-22 is associated with poor prognosis in cervical cancer. *Int J Clin Exp Pathol* 10: 9515-9520, 2017.
16. Xiong J, Du Q and Liang Z: Tumor-suppressive microRNA-22 inhibits the transcription of E-box-containing c-Myc target genes by silencing c-Myc binding protein. *Oncogene* 29: 4980-4988, 2010.
17. Grimson A, Farh KK, Johnston WK, Garrett-Engele P, Lim LP and Bartel DP: MicroRNA targeting specificity in mammals: Determinants beyond seed pairing. *Mol Cell* 27: 91-105, 2007.
18. Wong N and Wang X: MiRDB: An online resource for microRNA target prediction and functional annotations. *Nucleic Acids Res* 43 (Database Issue): D146-D152, 2015.
19. Livak KJ and Schmittgen TD: Analysis of relative gene expression data using real-time quantitative PCR and the 2(-Delta Delta C(T)) method. *Methods* 25: 402-408, 2001.
20. Ono YJ, Hayashi M, Tanabe A, Hayashi A, Kanemura M, Terai Y and Ohmichi M: Estradiol-mediated hepatocyte growth factor is involved in the implantation of endometriotic cells via the mesothelial-to-mesenchymal transition in the peritoneum. *Am J Physiol Endocrinol Metab* 308: E950-E959, 2015.
21. Franken NA, Rodermond HM, Stap J, Haveman J and van Bree C: Clonogenic assay of cells in vitro. *Nat Protoc* 1: 2315-2319, 2006.
22. Taira T, Maeda J, Onishi T, Kitaura H, Yoshida S, Kato H, Ikeda M, Tamai K, Iguchi-Ariga SM and Ariga H: AMY-1, a novel C-MYC binding protein that stimulates transcription activity of C-MYC. *Genes Cells* 3: 549-565, 1998.
23. Wu KJ, Grandori C, Amacker M, Simon-Vermot N, Polack A, Lingner J and Dalla-Favera R: Direct activation of TERT transcription by c-MYC. *Nat Genet* 21: 220-224, 1999.
24. Zhang W and Xing L: RNAi gene therapy of SiHa cells via targeting human TERT induces growth inhibition and enhances radiosensitivity. *Int J Oncol* 43: 1228-1234, 2013.
25. Nakatani F, Ferracin M, Manara MC, Ventura S, Del Monaco V, Ferrari S, Alberghini M, Grilli A, Knuutila S, Schaefer KL, *et al*: MiR-34a predicts survival of Ewing's sarcoma patients and directly influences cell chemo-sensitivity and malignancy. *J Pathol* 226: 796-805, 2012.
26. Lagos-Quintana M, Rauhut R, Lendeckel W and Tuschl T: Identification of novel genes coding for small expressed RNAs. *Science* 294: 853-858, 2001.
27. Xin M, Qiao Z, Li J, Liu J, Song S, Zhao X, Miao P, Tang T, Wang L, Liu W, *et al*: MiR-22 inhibits tumor growth and metastasis by targeting ATP citrate lyase: Evidence in osteosarcoma, prostate cancer, cervical cancer and lung cancer. *Oncotarget* 7: 44252-44265, 2016.
28. Li J, Liang S, Yu H, Zhang J, Ma D and Lu X: An inhibitory effect of miR-22 on cell migration and invasion in ovarian cancer. *Gynecol Oncol* 119: 543-538, 2010.
29. Zuo QF, Cao LY, Yu T, Gong L, Wang LN, Zhao YL, Xiao B and Zou QM: MicroRNA-22 inhibits tumor growth and metastasis in gastric cancer by directly targeting MMP14 and Snail. *Cell Death Dis* 6: e2000, 2015.
30. Zhang H, Tang J, Li C, Kong J, Wang J, Wu Y, Xu E and Lai M: MiR-22 regulates 5-FU sensitivity by inhibiting autophagy and promoting apoptosis in colorectal cancer cells. *Cancer Lett* 356: 781-790, 2015.
31. Zhang T, Xue X and Peng H: Therapeutic delivery of miR-29b enhances radiosensitivity in cervical cancer. *Mol Ther* 27: 1183-1194, 2019.
32. Pedroza-Torres A, Campos-Parra AD, Millan-Catalan O, Loissell-Baltazar YA, Zamudio-Meza H, Cantú de León D, Montalvo-Esquivel G, Isla-Ortiz D, Herrera LA, Angeles-Zaragoza Ó, *et al*: MicroRNA-125 modulates radioresistance through targeting p21 in cervical cancer. *Oncol Rep* 39: 1532-1540, 2018.
33. Zhang X, Li Y, Wang D and Wei X: MiR-22 suppresses tumorigenesis and improves radiosensitivity of breast cancer cells by targeting Sirt1. *Biol Res* 50: 27, 2017.
34. Liu Z, Li T, Deng S, Fu S, Zhou X and He Y: Radiation induces apoptosis and osteogenic impairment through miR-22-mediated intracellular oxidative stress in bone marrow mesenchymal stem cells. *Stem Cells Int* 2018: 5845402, 2018.
35. Sakamuro D and Prendergast GC: New Myc-interacting proteins: A second Myc network emerges. *Oncogene* 18: 2942-2954, 1999.
36. Wang H, Yan X, Ji LY, Ji XT, Wang P, Guo SW and Li SZ: MiR-139 functions as an antioncomir to repress glioma progression through targeting IGF-1 R, AMY-1, and PGC-1β. *Technol Cancer Res Treat* 16: 497-511, 2017.
37. Gong L, Xia Y, Qian Z, Shi J, Luo J, Song G, Xu J and Ye Z: Overexpression of MYC binding protein promotes invasion and migration in gastric cancer. *Oncol Lett* 15: 5243-5249, 2018.



This work is licensed under a Creative Commons Attribution-NonCommercial-NoDerivatives 4.0 International (CC BY-NC-ND 4.0) License.